



HAL
open science

Crystal Templating with Mutually Miscible Solvents: A Simple Path to Hierarchical Porosity

Christian Guizard, Jérôme Leloup, Sylvain Deville

► **To cite this version:**

Christian Guizard, Jérôme Leloup, Sylvain Deville. Crystal Templating with Mutually Miscible Solvents: A Simple Path to Hierarchical Porosity. *Journal of the American Ceramic Society*, 2014, 97 (7), pp.2020-2023. 10.1111/jace.12995 . hal-01133190

HAL Id: hal-01133190

<https://hal.science/hal-01133190>

Submitted on 18 May 2018

HAL is a multi-disciplinary open access archive for the deposit and dissemination of scientific research documents, whether they are published or not. The documents may come from teaching and research institutions in France or abroad, or from public or private research centers.

L'archive ouverte pluridisciplinaire **HAL**, est destinée au dépôt et à la diffusion de documents scientifiques de niveau recherche, publiés ou non, émanant des établissements d'enseignement et de recherche français ou étrangers, des laboratoires publics ou privés.

Crystal-Templating With Mutually Miscible Solvents: A Simple Path To Hierarchical Porosity

Christian Guizard[†], Jérôme Leloup, Sylvain Deville*

Laboratoire de Synthèse et Fonctionnalisation des Céramiques, UMR3080 CNRS/Saint-Gobain, Cavaillon, France

[†] now with Institut Européen des Membranes, Université de Montpellier 2, Place Eugène Bataillon, 34095 Montpellier cedex 5, France

* To whom correspondence should be addressed. E-mail: sylvain.deville@saint-gobain.com

Abstract: Ice templating, a route where ice crystals are used to template macroporosity, has been used to process a variety of materials with one level of macropores. We demonstrate here a variant of ice templating based on the solidification of mutually miscible solvents. The solidification of different phases, each defined by their own size and morphology, provides a simple one-step processing route for materials with hierarchical porosity defined by up to three levels of macroporosity. These concepts are demonstrated with both ceramic (yttria-stabilized zirconia) and polymer (polyvinyl alcohol) materials.

Introduction

Macroporous materials comprising pores at multiple scales are required for a number of applications involving mass transfer (filtration), heat transfer, or surface reactions (catalysis). Many approaches have been developed to obtain ceramic materials with a hierarchical porosity¹, such as extrusion² or ice templating³. They typically involve the presence of a macro- or mesopore former that is removed by a heat treatment. Such structures are usually defined by one level of macroporosity and meso- or microporosity. Ice templating is a well-established materials processing route suitable for making macroporous materials with a directional porosity⁴. When a solvent other than water is used, the more generic term “crystal-templating” might be used. The formation of the porosity is based on the templating effects of the solvent crystals, which thus define macroporosity on a size scale defined by the crystal size. The addition of organic pore formers^{5,6} can add an additional level of macroporosity, but a careful heat treatment step is still required to eliminate the large quantity of pore formers.

Here we demonstrate a variant of crystal-templating based on the solidification of mutually miscible solvents that is able to create macropores at several scales without the assistance of organic pore formers. The solidification of different phases, each of them defined by their own size and morphology, provide a simple one-step processing route for materials with hier-

archical porosity. We demonstrate the approach in the tert-butyl-alcohol (TBA)/water system using either a ceramic (8mol.% yttria-stabilized zirconia) or a polymer (polyvinyl alcohol). TBA is a solvent extensively investigated and used in the pharmaceuticals industry⁷ and its phase diagram with water (figure 1) is therefore well-known. In addition, its phase equilibria as a function of temperature and pressure are compatible with the usual ice templating conditions and equipment. The use of TBA in ice templating has already been largely documented⁸⁻¹⁰, although always in its pure form.

Materials and Methods

The following products were used: distilled water, TBA (Sigma-Aldrich), 8mol.% yttria-stabilized zirconia (TZ8Y, Tosoh, Japan), dispersants (Prox B03, a polyacrylate ammonium salt from Synthron, Levallois-Paris, France), and a binder (polyethylene glycol PEG6M sold by Merck or polyvinyl-butyril (PVB) from Sigma-Aldrich) that is required to hold particles together during the freeze-drying step and avoid collapse of the porous structure. The macroporous PVA samples were obtained using a PVA (PVA LL6036) from Wacker (Burghausen, Germany). The ceramic suspensions are prepared by mixing the ceramic powder, the dispersant, the binder and the mix of solvents in predefined ratios. For TBA content up to 40wt%, ProxB03 was used as a dispersant and PEG6M as a binder. For TBA content above 70wt%, no dispersant was used and PVB was used as a binder, since it easily dissolves in concentrated TBA suspensions. The suspension was then ball-milled for 10 hours. The PVA solution was obtained by dissolving the PVA in water under magnetic stirring for 24 hrs. The suspension or solution were poured into a PTFE mold and cooled from the bottom, using a liquid-nitrogen cooled copper rod. The cooling rates were adjusted through a thermocouple and a heater. Details of the experimental setup can be found in previous papers¹¹. This setup provides a fine control of the ice growth velocity, along the temperature gradient direction. Once freezing is completed, the samples were freeze-dried for at least 48 hrs. in a commercial freeze-dryer (FREE Zone 2.5Plus, Labconco, Kansas City, Missouri, USA) to ensure a complete removal of the ice and TBA (or water/TBA hydrates) crystals. Ceramic samples were densified by a high temperature sintering treatment, with a temperature rise at a rate of 180°C/h up to 500°C, holding a 500°C for 1 hr, up to 1350°C at 300°C/hr, steady stage of 3 hours at 1350°C, temperature decrease at a rate of 350°C/h to room temperature. Samples were cut, perpendicular to the direction of the temperature gradient, using a low-speed diamond saw, and cleaned in an ultrasound bath to remove the debris. SEM observations were performed using either a TM1000 from Hitachi. Pore diameters and volume were measured by mercury intrusion porosimetry (AutoPore IV 9500, Micromeritics) with applied pressures up to 200 MPa.

Results and discussion

Structures with a hierarchical porosity are obtained when the solidification path goes through several solidification events at different temperatures. The resulting porous structures are then defined at multiple scales (figure 2). The temperatures of the solidification events are all different, crystallization of the various phases will thus occur at different moments of the process, ensuring a progressive organization towards the final structure. The basic requirement for the solvents is that their solubility limit for particles is very low (which is the case for ice¹²), so that pure phases are grown and effectively reject all the particles in the inter-crystal space. The pores characteristics were assessed by mercury porosimetry (figure 2C). Three distinct peaks, related to the three types of pores, are clearly observed in the pore size distribution. The solidification being directional, the tortuosity of the macropores is minimal. The resulting structures have thus a hierarchical porosity with three types of macropores of different morphologies and dimensions. Finer macropores (0.5 μm) are formed by the arrangement of concentrated particles at the end of freezing. Since breakthrough of the interface in the interparticle space occurs before maximum particle packing¹³, we can expect the resulting pores to be larger than expected from the maximum packing.

The porosimetry results indicate good connectivity between the various pore size scales.

The structures obtained can be rationalized by considering the phase diagram (Figure 1) and the expected sequence of solidification events, and assuming that we are constantly close to the equilibrium during solidification. If the conditions are suitable (path b in Figure 1), ice crystals form first (large pores observed in Fig. 2A and B). As solidification proceeds, the TBA content in the liquid solution increases, until it reaches the eutectic point. A eutectic structure then forms, in the intercrystal space (smaller macropores observed in Fig. 2 A and B). The expected proportion of the relative crystals can be estimated using the lever rule. The lamellar spacing in eutectic structures is typically $1/10^{\text{th}}$ of that of dendrites grown under the same conditions¹⁴, which seems consistent with the current observations. An equivalent behavior can be obtained in the TBA-rich side of the phase diagram, for instance with a 5wt% water/95wt% TBA zirconia suspension. A hierarchical structure with two populations of macropores is obtained (Figure 2D). The largest macropores present a faceted morphology typical of TBA-templated materials¹⁵. The eutectic A in the water/TBA system (trajectory c in Figure 1) yields lamellar pores with a short spacing (1-3 μm , figure 3A), a range that has been difficult to achieve thus far in the other ice templating systems¹⁶. The pore size and morphology are thus consistent with that observed in Figure 2. If the TBA concentration is too low (4wt% of TBA, trajectory a in Figure 1), the fraction of particle in the liquid phase rejected in the intercrystal space is too high for any templating effect to occur. The concentration of particles is so high that they cannot rearrange when the eutectic is forming. The resulting structure comprises thus just two populations of macropores (Figure 3B), created respectively by the large ice crystals and the packing of particles. The final materials comprise polycrystalline platelets of large dimensions (10–20 μm in thickness, and hundreds of microns in length and width).

A variety of polymers have successfully been ice templated previously, including PVA¹⁷, cellulose¹⁸, hydrogels¹⁹, or composites²⁰. The concepts demonstrated here are generic, and we successfully prepared a macroporous polyvinyl alcohol (PVA) material exhibiting two levels of macroporosity (Figure 4). Large macropores (100-200 μm wide, hundreds of microns long) are separated by macroporous walls defined comprising smaller macropores (5-30 μm wide, 20-100 μm long). Both populations of macropores are continuous along the freezing direction.

Conclusions

Crystal-templating based on mutually miscible solvents is thus a versatile approach to obtain porous ceramic or polymer materials with a variety of pore morphologies, including hierarchical porosity with up to three levels of macroporosity. The principles demonstrated here are generic and can easily be extended to other systems with appropriate phase diagrams. The temperature and phase separation kinetics must nevertheless be compatible with the usual ice templating temperature and pressure conditions.

References

- ¹ P. Colombo, C. Vakifahmetoglu, and S. Costacurta, "Fabrication of ceramic components with hierarchical porosity," *J. Mater. Sci.*, **45** [20] 5425–5455 (2010).
- ² H. Yang, S. Yang, X. Chi, and J.R.G. Evans, "Fine ceramic lattices prepared by extrusion freeforming.," *J. Biomed. Mater. Res. B. Appl. Biomater.*, **79** [1] 116–21 (2006).
- ³ S.R. Mukai, H. Nishihara, and H. Tamon, "Formation of monolithic silica gel microhoneycombs (SMHs) using pseudosteady state growth of microstructural ice crystals.," *Chem. Commun.*, [7] 874–5 (2004).
- ⁴ S. Deville, "Ice-templating, freeze casting: Beyond materials processing," *J. Mater. Res.*, **28** [17] 2202–2219 (2013).
- ⁵ J.-W. Kim, K. Tazumi, R. Okaji, and M. Ohshima, "Honeycomb Monolith-Structured Silica with Highly Ordered, Three-Dimensionally Interconnected Macroporous Walls," *Chem. Mater.*, **21** [15] 3476–3478 (2009).
- ⁶ K. Zuo, Y. Zhang, Y.-P. Zeng, and D. Jiang, "Pore-forming agent induced microstructure evolution of freeze casted hydroxyapatite," *Ceram. Int.*, **37** [1] 407–410 (2011).
- ⁷ S. Vessot and J. Andrieu, "A Review on Freeze Drying of Drugs with tert -Butanol (TBA) + Water Systems: Characteristics, Advantages, Drawbacks," *Dry. Technol. An Int. J.*, **30** [4] 377–385 (2012).
- ⁸ R. Chen, C.-A. Wang, Y. Huang, L. Ma, and W. Lin, "Ceramics with Special Porous Structures Fabricated by Freeze-Gelcasting: Using tert-Butyl Alcohol as a Template," *J. Am. Ceram. Soc.*, **90** [11] 3478–3484 (2007).
- ⁹ L. Hu, C.-A. Wang, Y. Huang, C. Sun, S. Lu, and Z. Hu, "Control of pore channel size during freeze casting of porous YSZ ceramics with unidirectionally aligned channels using different freezing temperatures," *J. Eur. Ceram. Soc.*, **30** [16] 3389–3396 (2010).
- ¹⁰ T.Y. Yang, H.B. Ji, S.Y. Yoon, B.K. Kim, and H.C. Park, "Porous mullite composite with controlled pore structure processed using a freeze casting of TBA-based coal fly ash slurries," *Resour. Conserv. Recycl.*, **54** [11] 816–820 (2010).

- ¹¹ S. Deville, E. Saiz, and A.P. Tomsia, "Ice-templated porous alumina structures," *Acta Mater.*, **55** [6] 1965–1974 (2007).
- ¹² J.A.W. Elliott and S.S.L. Peppin, "Particle Trapping and Banding in Rapid Colloidal Solidification," *Phys. Rev. Lett.*, **107** [16] 168301 (2011).
- ¹³ S. Deville and G. Bernard-Granger, "Influence of surface tension, osmotic pressure and pores morphology on the densification of ice-templated ceramics," *J. Eur. Ceram. Soc.*, **31** [6] 983–987 (2011).
- ¹⁴ W. Kurz and D.J. Fisher, *Fundamentals of Solidification*. Trans Tech Publications Ltd, 1989.
- ¹⁵ D. Li and M. Li, "Preparation of porous alumina ceramic with ultra-high porosity and long straight pores by freeze casting," *J. Porous Mater.*, **19** [3] 345–349 (2011).
- ¹⁶ T. Waschkies, R. Oberacker, and M.J. Hoffmann, "Investigation of structure formation during freeze-casting from very slow to very fast solidification velocities," *Acta Mater.*, **59** [13] 5135–5145 (2011).
- ¹⁷ H. Zhang, I. Hussain, M. Brust, M.F. Butler, S.P. Rannard, and A.I. Cooper, "Aligned two- and three-dimensional structures by directional freezing of polymers and nanoparticles.," *Nat. Mater.*, **4** [10] 787–93 (2005).
- ¹⁸ R. Dash, Y. Li, and A.J. Ragauskas, "Cellulose nanowhisker foams by freeze casting," *Carbohydr. Polym.*, **88** [2] 789–792 (2012).
- ¹⁹ J. Zhu, J. Wang, Q. Liu, Y. Liu, L. Wang, C. He, and H. Wang, "Anisotropic tough poly(2-hydroxyethyl methacrylate) hydrogels fabricated by directional freezing redox polymerization," *J. Mater. Chem. B*, **1** [7] 978 (2013).
- ²⁰ H.E. Romeo, C.E. Hoppe, M.A. López-Quintela, R.J.J. Williams, Y. Minaberry, and M. Jobbágy, "Directional freezing of liquid crystalline systems: from silver nanowire/PVA aqueous dispersions to highly ordered and electrically conductive macroporous scaffolds," *J. Mater. Chem.*, **22** [18] 9195 (2012).

Figure

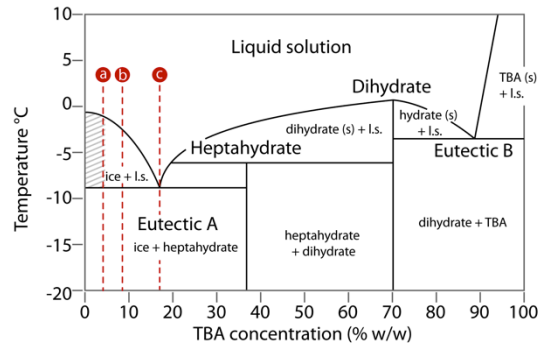


Figure 1. Phase diagram of the TBA/water system, after Vessot and Andrieu⁷. Depending on the relative concentration of water and TBA in the slurry, different types of structure may be processed, including hierarchical structures obtained with two types of crystals. The dashed area indicates the region where the TBA concentration is too low to obtain hierarchical architectures: the fraction of particle in the liquid phase rejected in the intercrystal space is too high for any templating effect to occur. The same behavior happens on the TBA-rich side of the phase diagram (dashed area not shown for clarity). The different trajectories (a, b, c) are discussed in the text.

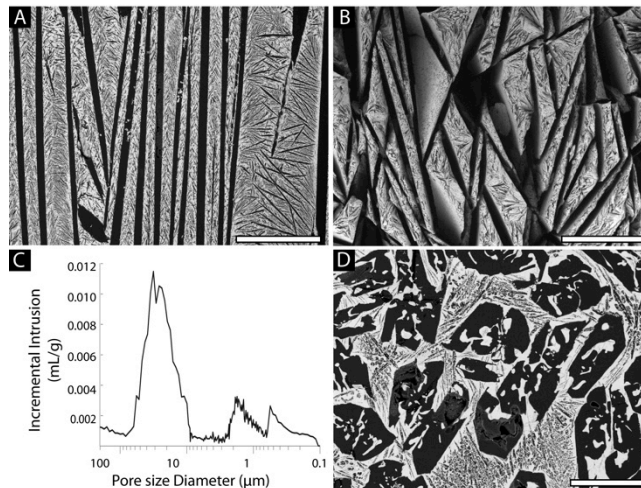


Figure 2. TZ8Y porous structure with hierarchical porosity obtained from either 84wt% water/16wt% TBA (A-B) or 5wt% water/95wt% TBA (D). SEM micrographs parallel (A) or perpendicular (B, D) to the freezing direction, and pore size distribution (C) from mercury porosimetry intrusion for the 84wt% water/16wt% TBA sample. Cooling rates: 2°C/min. The cross-sections shown in A and D were obtained after infiltration with an epoxy resin and polishing. Scale bars: A, B: 500μm, C: 150μm.

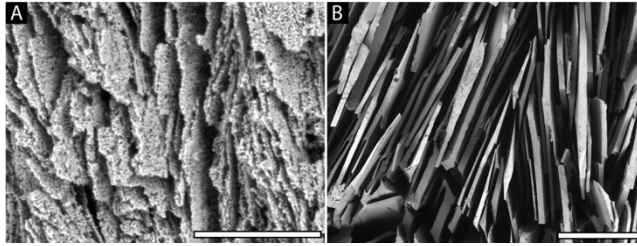


Figure 3. SEM micrographs of the different types of porous, non-hierarchical TZ8Y structures obtained. Cross-section perpendicular to the freezing direction. (A) 80wt% water/20wt% TBA (close to eutectic composition) (B) 95wt% water/5wt% TBA . Scale bars: A: 30 μ m, B: 500 μ m.

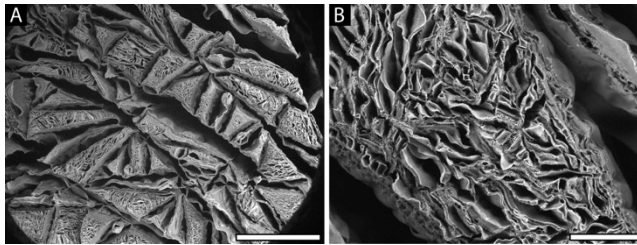


Figure 4. PVA porous structure with two levels of porosity (84wt% water/16wt% TBA). SEM micrographs perpendicular to the freezing direction. (B) Close-up view showing the finer macropores. Cooling rate: 2 $^{\circ}$ C/min. Scale bars: A: 1mm, B: 150 μ m.